PERGAMON

International Journal of Multiphase Flow 26 (2000) 877–887

International Journal of Multiphase Flow

www.elsevier.com/locate/ijmulflow

Brief communication

Hydrodynamic interactions between two identical spheres held fixed side by side against a uniform stream directed perpendicular to the line connecting the spheres' centres

R. Folkersma[a,*], H.N. Stein[a], F.N. van de Vosse[b]

[a]*Laboratory of Colloid Chemistry and Thermodynamics, Department of Chemical Engineering, Eindhoven University of Technology, P.O. Box 513, 5600 MB Eindhoven, The Netherlands*

[b]*Computational and Experimental Mechanics, Faculty of Mechanical Engineering, Eindhoven University of Technology, P.O. Box 513, 5600 MB Eindhoven, The Netherlands*

Received 20 May 1998; received in revised form 1 June 1999

Abstract

Hydrodynamic interactions between two identical solid spheres are investigated numerically using a finite element method. The spheres are held fixed relative to each other with the line connecting their centres normal to the flow direction. The method is applied in three-dimensional, at Reynolds numbers 10, 50 and 5×10^{-7}. The drag and interaction coefficients of the spheres are calculated as functions of the distance between the two spheres. The results of the calculations show that, for Reynolds number of 50, the two spheres are repelled when the spacing is of the order of the diameter but are weakly attracted at intermediate separation distances. The results agree with experimental and theoretical data reported for different Reynolds numbers. © 2000 Elsevier Science Ltd. All rights reserved.

Keywords: Hydrodynamic interactions; Finite element method; Sedimentation; Gravity

1. Introduction

This paper originated from experimental work we performed on aggregation experiments on dispersions consisting of polystyrene spheres and water (Folkersma et al., 1998; Folkersma and Stein, 1998). We studied the influence of gravity on Brownian coagulation and found an

* Corresponding author.

0301-9322/00/$ - see front matter
PII: S0301-9322(99)00067-1

increase in coagulation rate at micro-g conditions compared to 1g conditions. One explanation for this behaviour could be an influence of hydrodynamics: at 1g conditions the polystyrene spheres sediment and hydrodynamic interactions between two spheres approaching each other, might retard coagulation. At micro-g conditions these hydrodynamic interactions are absent, because at micro-g the particles do not settle.

The intention of this investigation is to study the influence of the non-linear terms of the Navier–Stokes equation on the hydrodynamic interaction forces between two settling spheres at 1g conditions. Among the possible types of hydrodynamic interaction, especially of interest in the present study is the hydrodynamic interaction of two particles sedimenting side by side. For incompressible fluids with constant viscosity neglecting inertial effects, the transport equation is the Stokes equation; its solution can be found in an analytical form if the geometry of the considered particles is such that coordinate surfaces fit the physical boundaries of the problem. Examples of this approach include the classical problem of a single spherical particle in a uniform flow, solved by Stokes (1851), and ellipsoidal or two spherical particles which are close together in a linear flow, discussed by Stimson and Jefferey (1926). These analytical solutions, however, are restricted to Reynolds numbers $Re < 3$ (particle diameter as the characteristic length and the flow velocity at a large distance as the characteristic velocity). So for flows at low Reynolds numbers (10^{-7}–10^{-5}), which are common in stagnant colloid dispersions, normally Stokes law applies; however, for flows at intermediate Reynolds numbers, which are common in the processing of colloids (transportation, dispersing of particles in colloid or pearl mills, stirred vessels etc.) it is necessary to solve the Navier–Stokes equations numerically. Many investigators have considered the interactions between particles and the surrounding fluid by analytical and numerical methods. Among them are Eveson et al. (1959), Hocking (1964), Jayaweera et al. (1964), Goldman et al. (1996), Wakiya (1967), O'Neill (1969), O'Neill and Majumdar (1970), Batchelor (1972), Batchelor and Green (1976), Davis et al. (1976), Jeffrey (1982), Dabros (1985), Kim and Mifflin (1985), Yoon and Kim (1987), Cichocki et al. (1988, 1994) and Kim et al. (1993).

Kim et al. (1993) studied the three-dimensional (3D) flow over two identical spheres which are held fixed relative to each other with the line connecting their centres normal to uniform stream, for $Re = 50$, 100 and 150. The two spheres *repel* each other when they are close, and the repulsion is stronger the closer they are. On the other hand, the two spheres weakly *attract* each other at intermediate separation distances.

Although, recently, some numerical studies have been performed for 3D flows over a single sphere by Dandy and Dwyer (1990) and Tomboulides et al. (1991), 3D flow interactions between particles have not been studied extensively, to the knowledge of the author, with the exception of Kim et al. (1993), Cichocki et al. (1994), Joseph and Liu (1993) and Joseph et al. (1994).

In the present paper, flow interactions were calculated between two identical spheres which are held fixed side by side against a uniform stream directed perpendicular to the line connecting the spheres' centres, at different Reynolds numbers. The effects of 3D interactions on the drag and interaction coefficients were calculated as a function of the dimensionless distance between the two spheres and Reynolds number by a finite element method (FEM) (Cuvelier et al., 1986), using Cartesian coordinates. The drag coefficients were also calculated for verification of our program and comparison with results of other investigators. However, these calculations will not be treated in the present paper. The interaction coefficients calculated in this paper indicate whether the particles repel or attract each other.

The novelties of this paper are: (i) the use of 3D Cartesian coordinates for sphere calculations; (ii) investigation whether spheres repel or attract each other at low Reynolds numbers, without ignoring the non-linear terms in the Navier–Stokes equations; (iii) our computational domain can be easily extended to multiple-particle interactions, which are very important in colloids. Because of the simple cube geometry of the computational domain for one sphere used in this paper, we can create a 3D computational domain with as many spheres as one would like to have.

2. Governing equations and computational method

2.1. Governing equations

To calculate the velocity profile of the continuous phase, Cartesian coordinates are used. The equations governing the flow are:

(a) the continuity equation, i.e., mass balance for a small volume element of fluid, at constant density ρ,

$$\nabla \cdot \underline{u} = 0 \tag{1}$$

and
(b) the momentum equation for steady Newtonian flows:

$$\rho(\underline{u} \cdot \nabla) - \nabla \cdot \sigma = \rho \underline{f} \tag{2}$$

with

$$\sigma = -pI + \tau \tag{3}$$

with

$$\tau = \eta\left(\nabla \underline{u} + (\nabla \underline{u})^c\right) \tag{4}$$

Here I is the unit tensor, σ is the Cauchy stress tensor, τ is the viscous stress tensor, η is the viscosity, $\underline{u}$ is the velocity of the fluid phase, p is the pressure and $\underline{f}$ is an external volume force per unit of mass.

These equations can be written in a dimensionless form by introducing a characteristic length L and a characteristic scalar velocity U_0, and using the following definitions:

$$x' = \frac{x}{L}, \quad \underline{u}' = \frac{u}{U_0}, \quad p' = \frac{p}{\rho U_0^2}, \quad \underline{f}' = \frac{f}{U_0^2/L} \tag{5}$$

Omitting the primes, we obtain:

$$\nabla \cdot \underline{u} = 0 \tag{6}$$

and

$$-\frac{1}{Re}\Delta\underline{u}+(\underline{u}\cdot\nabla)\underline{u}+\nabla p=\underline{f} \tag{7}$$

where Re is the Reynolds number defined by $Re=\rho U_0 L/\eta$.

$\underline{f}$ is set equal to zero in our calculations, because gravity is introduced as the settling rate of the particles which is expressed in the Reynolds number.

2.2. Problem statement and numerical solution method

The calculations described in this paper are based on the following experimental system (Folkersma et al., 1998):

- Polystyrene spheres with a radius of 1 μm and a density of 1.050 kg/m^3; the velocity of the particles during settling at terrestrial conditions varied from 10^{-7} to 10^{-6} m/s; no settling at micro-g conditions.
- The fluid used was water, with a density of 999.698 kg/m^3 and a viscosity of 10^{-3} Pa s (during the experiments the density of the continuous phase was adapted by adding deuterium oxide (D_2O)).

The characteristic length in the calculations is chosen to be equal to the particle diameter. At the inlet of the calculation domain a constant velocity (independent of distance measured from the side faces of the computational domain) is assumed (see Fig. 1). The characteristic velocity U_0 is defined as the value of this constant velocity.

The 3D computational domain in our calculations contains one sphere. As a computational domain a cube is taken and the sphere is placed at the centre of this cube.

For the calculation of the flow around two spheres a symmetry condition is used at one side of this cube. The sides of the numerical box are 24 times the diameter of a sphere. For the two spheres problem, boundary S3 (shaded plane in Fig. 1) is shifted in the x-direction to obtain the needed separation distance between the two spheres. The sides of the numerical box are 48 times as large as the smallest separation distance between the spheres. The numerical box

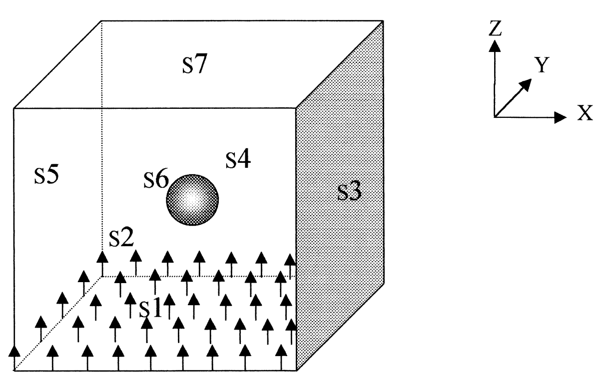

Fig. 1. Computational domain and boundary conditions for the calculation of the hydrodynamic force acting on two spheres placed side by side.

contains 6000 elements, corresponding with 58,000 nodes, with a higher density of nodes on the sphere surface and in the proximity of the sphere, than at the boundaries of the numerical box. The size and the spatial resolution of the numerical box were tested and with the specifications given in this section no wall effect of the numerical box on the results of the calculations was found.

Fig. 1 shows the computational domain together with the inflow conditions. In this domain the following physical situation has been simulated.

2.2.1. One sphere in the domain and one other sphere in an adjacent domain

The tangential components, in normal direction, of the velocity with respect to one side face are made equal to zero and on the other five side faces the dimensionless velocity is equal to U_0 in the z-direction, hence for the calculation of two spheres, only one sphere domain needs to be considered. Because of the symmetry the following boundary condition holds for the calculations of two spheres (boundary S3):

$$u_x = 0,\ \delta_{xy} = \delta_{xz} = 0. \tag{8}$$

2.3. Calculation of the non-dimensional drag and interaction coefficients

The non-dimensional drag and interaction coefficients are evaluated from the drag and interaction forces F_D and F_I:

$$F_\mathrm{D} = \int_S -p\underline{n}\cdot\underline{e}_z\,\mathrm{d}S + \int_S \underline{n}\cdot\underline{\underline{\tau}}\cdot\underline{e}_z\,\mathrm{d}S, \tag{9}$$

$$F_\mathrm{I} = \int_S -p\underline{n}\cdot\underline{e}_x\,\mathrm{d}S + \int_S \underline{n}\cdot\underline{\underline{\tau}}\cdot\underline{e}_x\,\mathrm{d}S, \tag{10}$$

where $\underline{e}_x$ and $\underline{e}_z$ denote the unit vectors in x- and z-direction, S denotes the surface of the sphere, n is the outward unit normal vector at the surface and $\underline{\underline{\tau}}$ is the viscous stress tensor.

So to calculate the drag force, F_D the z-components of the normal and tangential stress, at the particle surface need to be integrated over the particle surface. To calculate the interaction force, the x-components of the normal and tangential stress at the particle surface need to be integrated over the particle surface. Non-dimensional coefficients of drag and interaction are defined, respectively, as:

$$C_\mathrm{D} = \frac{F_\mathrm{D}}{\left(\frac{1}{2}\rho U_0^2 d^2\right)}, \tag{11}$$

$$C_\mathrm{I} = \frac{F_\mathrm{I}}{\left(\frac{1}{2}\rho U_0^2 d^2\right)}, \tag{12}$$

where ρ is the density of the particle. The factor $\frac{1}{2}$ has no role in the non-dimensionalisation, but is conventionally included because $\frac{1}{2}\rho U_0^2$ has physical significance (dynamic pressure) in Bernoulli's equation (Tritton, 1988); d is equal to the non-dimensional particle diameter. At low Reynolds numbers, the Stokes law applies and the drag coefficient for a sphere equals:

$$C_D = \frac{6\pi}{Re} \tag{13}$$

2.4. Calculation of the 3D flow around two spheres placed side by side

A steady 3D incompressible laminar flow was considered of a Newtonian fluid past two identical spheres held fixed, with the line connecting the sphere centres normal to a uniform stream, as shown in Fig. 2. First, we test the accuracy of the full 3D solution procedure by predicting the flow over a single sphere. Then, we discuss the 3D flow interactions between two spheres.

The calculations were performed on a Power Challenge XL (Silicon Graphics) computer, the calculation time varied between 8 and 10 CPU (Compiler Processing Units) hours for every single calculation. The finite elements software package was developed by the Engineering office SEPRA (Segal, 1993).

3. Results and discussion

3.1. Flow interactions of two spheres

We have calculated two values for C_D in the case of two spheres. For $d_0 = 1.50$ and 2.31,

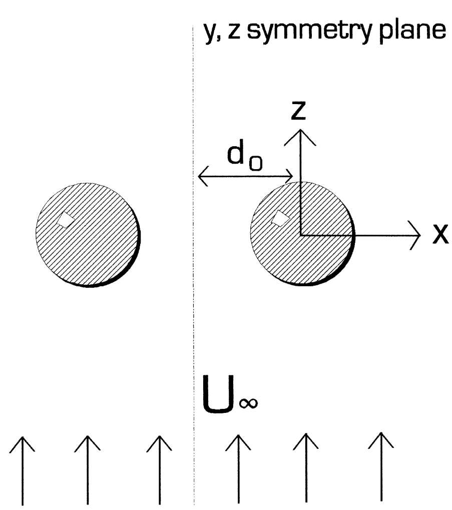

Fig. 2. Flow geometry and coordinates, d_0 is the distance normalized by the sphere radius from a sphere centre to the symmetry plane between two spheres.

$C_D = 4.87$ and 4.53 for $Re = 10$ and 1.74 and 1.69 for $Re = 50$. For $d_0 > 4$, C_D is equal to the values prevailing in the case of one sphere. For $Re = 50$, the results of Kim et al. (1993) differ by less than 3% from our data.

Fig. 3 shows the interaction coefficient as a function of d_0 (the distance normalised by the sphere radius) at $Re = 10$ and 50. The interaction coefficient C_I is negative for $d_0 < 23$ for $Re = 10$ (repulsion). It is also negative for $d_0 < 7.9$ and $Re = 50$. On the other hand at intermediate separation distances, C_I is positive and relatively small; that is, the two spheres weakly attract each other. This is the case for $7.9 < d_0 < 21$ at $Re = 50$. When $d_0 > 21$, however, the interaction vanishes for both Reynolds numbers.The interaction force vanishes at a separation of 23 radii, which is not a box-size effect. From the plot of Kim et al. (1993), we can conclude that their data are within 5% of our results.

The interaction coefficients were calculated as a function of d_0 for $Re = 5 \times 10^{-7}$, which prevailed in our experiments (Folkersma et al., 1998). When d_0 equals 1.5 and 2.3, the interaction coefficient is 73×10^3 and 50×10^3, respectively. This corresponds to the repulsive interaction force (F_I) of 9.1×10^{-18} and 6.2×10^{-18} N, respectively. These forces are very small (compared with the drag force and London–van der Waals attraction, 10^{-15} and 10^{-14} N, respectively), even at those small separation distances. Therefore, *no* retarding of coagulation at 1g due to hydrodynamic interactions is expected.

3.2. Flow structure around two spheres

Figs. 4 and 5 show the streamlines for two spheres at $d_0 = 1.5$ for $Re = 50$ and 5×10^{-7}.

At $Re = 5 \times 10^{-7}$, the streamline pattern does not deviate significantly from the Stokes flow pattern. Viscous effects dominate at any separation distance, and the spheres weakly *repel* each other at all separations.

At $Re = 50$, partial blockage of the flow in the space between the spheres causes a different flow pattern (Fig. 6). Far from the spheres, the stagnation streamlines are closer to the symmetry plane; the same holds for the stagnation points on the sphere surfaces A, but to a

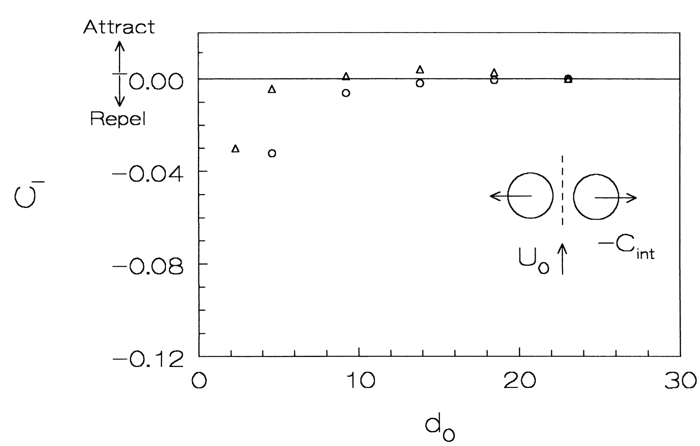

Fig. 3. Calculated interaction coefficients (C_I) of the solid spheres as a function of d_0 at $Re = 10$ (○) and $Re = 50$ (△).

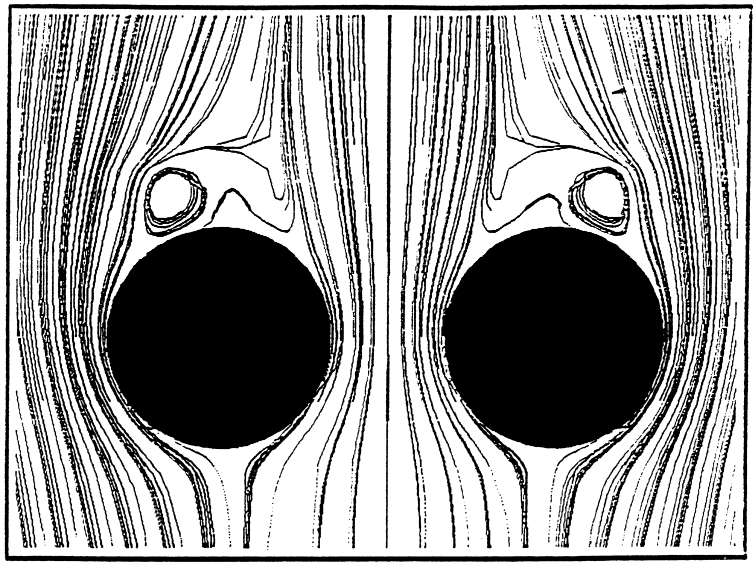

Fig. 4. Streamlines around two spheres in the principal plane at $Re = 50$ and $d_0 = 1.5$.

lesser degree. Thus, the stagnation streamlines diverge and this causes flow accelerations near the spheres, which in turn cause changes in the local pressure and shear stress. For the left sphere (Fig. 6), at A and C, a higher pressure is generated than at B and D, respectively. However, not all these effects are of equal importance for the interaction between the spheres.

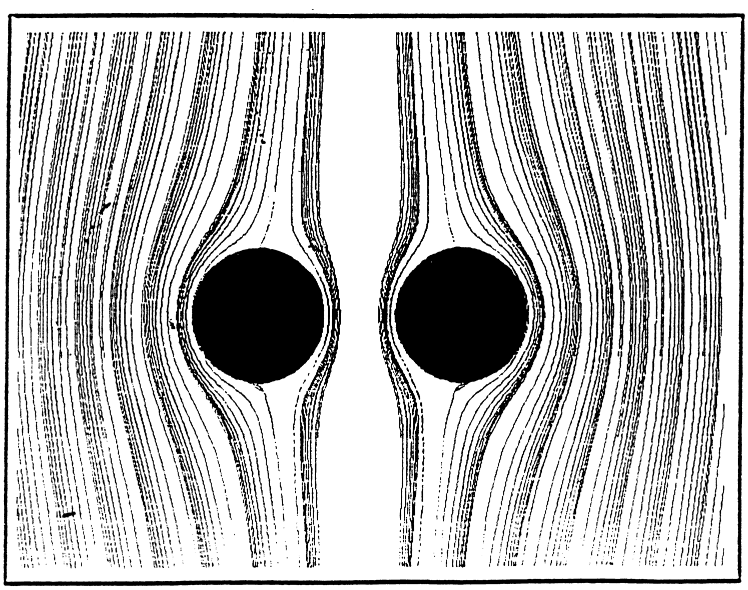

Fig. 5. Streamlines around two spheres in the principal plane at $Re = 5 \times 10^{-7}$ and $d_0 = 1.5$.

Thus, the shear stresses at C and D are directed normally to the line connecting the spheres' centres and do not contribute attraction or repulsion.

The resulting force has the following characteristics: when the spheres are very close, the effects of pressures and shear stresses at points A and B dominate over those at C and D; the net effect is that the spheres *repel* each other. When the spheres are at intermediate distances, the effects at C and D dominate slightly, and the spheres experience a weak *attraction* (see Fig. 3).

According to Kim et al. (1993), the torque acting on the sphere is relatively small, and the moment coefficient (defined as: $M = \int_S r x \underline{\tau}\, \mathrm{d}S$, where S denotes the surface of the sphere, r is the position vector from the centre of the sphere, and $\underline{\tau}$ is the viscous stress tensor) is less than 1% of the drag coefficient for all the separation distances and Reynolds numbers. According to Kim et al. (1993), the main reason for this is that the torque depends only on the distribution of the shear stresses and it appears that the shear stress on one side of the sphere counteracts the stress on the other side of the sphere. Therefore, no effect on the interaction coefficients is expected due to rotation of the spheres.

4. Conclusions

Interaction forces were calculated by a 3D FEM, for the case of two spherical particles in a flow directed perpendicular to the line connecting their centres. The method was tested by calculating Stokes flow at $Re < 3$, and Navier–Stokes flow at $Re > 3$ around a single spherical particle. The results (not shown here), were in good agreement with data found in literature (Stimson and Jefferey, 1926; Happel and Brenner, 1965; Ossen, 1927).

The calculations of flow interactions between two spheres, yield negative interaction coefficient $C_{\rm I}$ for $d_0 < 23$, $Re = 10$ (repulsion). $C_{\rm I}$ is also negative for $d_0 < 8$, $Re = 50$. On the other hand, $C_{\rm I}$ is positive and relatively small, that is, the two spheres weakly attract each other at intermediate separation distances: $8 < d_0 < 21$ and $Re = 50$. When $d_0 > 21$ the

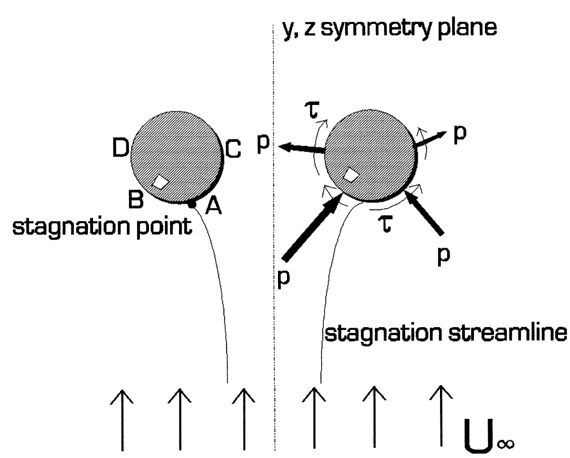

Fig. 6. Pressure (p) and shear stress (τ) acting on the spheres for $Re = 50$ at $d_0 = 1.5$.

interaction vanishes for all Reynolds numbers. The results agreed with those found by Kim et al. (1993).

For $Re = 5 \times 10^{-7}$, when $d_0 = 1.5$, $C_I = 73{,}000$. This corresponds to repulsive interaction force of 9×10^{-18} N. This force is four orders of magnitude lower than the drag force and London–van der Waals attraction force. It should be noted that the van der Waals forces are significant at shorter interaction distances than those calculated in the case of $d_0 = 1.5$. However, at smaller values of d_0 the repulsive hydrodynamic interaction is much less than the London–van der Waals attraction force. When two spheres are almost in contact, the flow considers the two spheres as one object and there are no stress and pressure gradients in the gap between them.

We conclude that no significant retarding of coagulation at 1g, during particles' settling, is expected resulting from these small repulsive hydrodynamic interaction forces.

Acknowledgements

The financial support of the 'Space Research Organisation Netherlands' is gratefully acknowledged.

References

Batchelor, G.K., 1972. Sedimentation in a dilute dispersion of spheres. J. Fluid Mech 52, 245–268.

Batchelor, G.K., Green, J.T., 1976. The hydrodynamic interaction of two small freely-moving spheres in a linear flow field. J. Fluid Mech 56, 375–400.

Cichocki, B., Felderhof, B.U., Schmitz, R., 1988. Hydrodynamic interactions between two spherical particles. Physico Chem. Hyd 10, 383–403.

Cichocki, B., Felderhof, B.U., Hinsen, K., Wajnryb, E., Blawzdziewicz, J., 1994. Friction and mobility of many spheres in Stokes flow. J. Chem. Phys 100, 3780–3790.

Cuvelier, C., Segal, A., van Steenhoven, A.A., 1986. Finite Element Methods and Navier–Stokes Equations. Reidel, Dordrecht, The Netherlands.

Dabros, T., 1985. A singularity method for calculating hydrodynamic forces and particle velocities in low-Reynolds-number flows. J. Fluid Mech 156, 1–21.

Dandy, D.S., Dwyer, H.A., 1990. A sphere in shear flow at finite Reynolds number: effect of shear on particle lift, drag, and heat transfer. J. Fluid Mech 216, 381–410.

Davis, A.M.J., O'Neill, M.E., Dorrepaal, J.M., Ranger, K.B., 1976. Separation from the surface of two equal spheres in Stokes flow. J. Fluid Mech 77, 625–644.

Eveson, G.F., Hall, E.W., Ward, S.G., 1959. Interaction between two equal-sized equal-setting spheres moving through a viscous fluid. Brit. J. Appl. Phys 10, 43–47.

Folkersma, R., van Diemen, A.J.G., Stein, H.N., 1998. Influence of gravity on perikinetic coagulation. Part I: experimental. J. Colloid Interface Sci 206, 482–493.

Folkersma, R., Stein, H.N., 1998. Influence of gravity on perikinetic coagulation. Part II: theoretical analysis. J. Colloid Interface Sci 206, 494–504.

Goldman, A.J., Cox, R.G., Brenner, H., 1996. The slow motion of two identical arbitrarily oriented spheres through a viscous fluid. Chem. Eng. Sci 21, 1151–1170.

Happel, J., Brenner, H., 1965. Low Reynolds Number Hydrodynamics. Nijhoff, Dordrecht.

Hocking, L.M., 1964. The behaviour of clusters of spheres falling in a viscous fluid. Part II: slow motion theory. J. Fluid Mech 20, 129–139.

Jayaweera, K.O.L.F., Mason, B.J., Slack, G.W., 1964. The behaviour of clusters of spheres falling in a viscous fluid. Part I: experiment. J. Fluid Mech 20, 121–128.

Jeffrey, D.J., 1982. Low-Reynolds-number flow between converging spheres. Mathematika 29, 58–66.

Joseph, D.D., Liu, Y.L., 1993. Sedimentation of particles in polymer solutions. J. Fluid Mech 225, 565–595.

Joseph, D.D., Liu, Y.L., Poletto, M., Feng, J, 1994. J. Non. Newtonian Fluid Mech 54, 45–86.

Kim, I., Elghobashi, S., Sirignano, W.A., 1993. Three-dimensional flow over two spheres placed side by side. J. Fluid Mech 246, 465–488.

Kim, S., Mifflin, R.T., 1985. The resistance and mobility functions of two equal spheres in low-Reynolds-number flow. Phys. Fluids 28, 2033–2045.

O'Neill, M.E., Majumdar, S.R., 1970. Asymmetrical slow viscous fluid motions caused by the translation or rotation of two spheres. Part II: asymptotic form of the solutions when the minimum clearance between the spheres approaches zero. Z.A.M.P 21, 180–187.

O'Neill, M.E., 1969. On asymmetrical slow viscous flows caused by the motion of two equal spheres almost in contact. Proc. Camb. Phil. Soc 65, 543–556.

Ossen, C.W., 1927. Hydrodynamik. Akademische Verlag, Leipzig.

Segal, A., 1993. Programmers Guide (Sepra analysis). Engineering Office Sepra, The Netherlands.

Stimson, M., Jefferey, G.B., 1926. The motion of two spheres in a viscous fluid. Proc. R. Soc. Lond A 111, 110–116.

Stokes, G.G, 1851. Trans. Camb. Phil. Soc 9, 8.

Tomboulides, Orszag, A.G., Karniadakis, S.A., 1991. Int. Soc. Offshore Polar Engng. Proc.

Tritton, D.J., 1988. Physical Fluid Dynamics. Clarendon Press, Oxford.

Wakiya, S., 1967. Slow motions of a viscous fluid around two spheres. J. Phys. Soc. Japan 22, 1101–1109.

Yoon, B.J., Kim, S., 1987. Note on the direct calculation of mobility functions for two equal-sized spheres in Stokes flow. J. Fluid Mech 185, 437–446.